



EUROfusion

EUROFUSION WPBOP-PR(16) 16678

J.I. Linares Hurtado et al.

Recuperated versus single recuperator re-compressed supercritical CO2 Brayton power cycles for DEMO fusion reactor based on Dual Coolant Lithium Lead blanket

Preprint of Paper to be submitted for publication in
Energy



This work has been carried out within the framework of the EUROfusion Consortium and has received funding from the Euratom research and training programme 2014-2018 under grant agreement No 633053. The views and opinions expressed herein do not necessarily reflect those of the European Commission.

This document is intended for publication in the open literature. It is made available on the clear understanding that it may not be further circulated and extracts or references may not be published prior to publication of the original when applicable, or without the consent of the Publications Officer, EUROfusion Programme Management Unit, Culham Science Centre, Abingdon, Oxon, OX14 3DB, UK or e-mail Publications.Officer@euro-fusion.org

Enquiries about Copyright and reproduction should be addressed to the Publications Officer, EUROfusion Programme Management Unit, Culham Science Centre, Abingdon, Oxon, OX14 3DB, UK or e-mail Publications.Officer@euro-fusion.org

The contents of this preprint and all other EUROfusion Preprints, Reports and Conference Papers are available to view online free at <http://www.euro-fusionscipub.org>. This site has full search facilities and e-mail alert options. In the JET specific papers the diagrams contained within the PDFs on this site are hyperlinked

designs may be explored for those walls that would work as discrete limiters during the limiter phase [7][1]. Of course, since they feature thick tungsten armour the penalty for such HHF designs is an overall reduction of reactor tritium breeding ratio (TBR). However, for those areas of FW with a moderate HHF (i.e., $>2\text{MW}/\text{m}^2$), a sufficient reactor TBR may be maintained by proposing a de-coupled concept based on splitting the wall into plasma-facing units or *fingers*. The work presented here is focused on this proposal.

The following list of potential advantages justifies the effort of exploring the de-coupled FW design based on fingers:

- Lower thermal stress compared to the baseline FW (the baseline being the integrated FW, which is the BB module box front face);
- Lower eddy currents during disruptions;
- Compatible with medium/high heat fluxes and keeping high TBR contribution behind the FW;
- Presents the possibility of a non-Eurofer structural material (e.g. a Cu alloy), which could improve FW power handling;
- The BB module is isolated from potentially destructive plasma events, and in the event of a failure of the FW the (high investment) BB module could be salvaged;
- FW no longer needs to be designed for the in-box LOCA load case, which for the integrated FW can be a design driver;
- Separation of the highly loaded FW and the tritium-containing BB could lead to an improved plant safety case.

1.2. Overall FW requirements and design study approach

A DEMO FW design proposal has to meet the following requirements:

- Survive a high heat flux (to be determined, and depends on location around the wall);
- Reduced activation materials and coolants;
- Structural materials must maintain good strength properties under the expected radiation environment;
- The plasma-facing armour material (here assumed to be tungsten) must offer good impurity control, low physical and chemical erosion and low tritium permeation;
- Survive electromagnetic loads and transient events (e.g., disruption load case), magnitude and frequency to be determined;
- Operating temperatures in structural material kept within material limits. For the purpose of this work we take the Eurofer allowable operating temperature range to be 300 to 550°C.

This list of requirements is broad, so at this stage it is necessary to develop a methodology that allows efficient exploration of different concepts. This requires analyses which are computationally inexpensive but sufficiently realistic to capture the design trends. Subsequently the most interesting proposals will be studied in more detail with specific assessments including consideration of a greater range of load cases and failure modes. Before describing the de-coupled FW design concept, an analysis tool supporting this activity is introduced in the following Section.

2. THAMES: Thermo-Hydraulic Analysis Model for heat flux Exposed Surfaces

2.1. Tool description

Correct thermo-hydraulic modelling is one of the key aspects in the design of a high heat flux plasma facing component (PFC). The final thermal and mechanical performance of the component is directly related to the definition of the coolant conditions and how the coolant properties evolve at each position of the cooling channels. Coolant medium, velocity, temperature, pressure at each position, pressure drop and heat transfer coefficients (HTCs) are all key variables for proposing feasible FW designs.

A new tool has been developed to support the FW design activity by providing all the necessary thermo-hydraulic information and linking it with preliminary thermal and mechanical finite element analysis of each explored conceptual PFC design. This tool, called Thermo-Hydraulic Analysis Model for heat flux Exposed Surfaces (THAMES), is particularly suited to rapid exploratory design/scoping studies of different de-coupled FW options. It consists on a 1-D finite difference Python code where thermo-hydraulic correlations are used to calculate coolant parameters which are then used as boundary conditions in linked 2-D or 3-D FE analyses. The benefits are:

- For a given geometry and coolant inputs, calculation of the coolant regime (pressure drop, temperature, velocity), heat transfer coefficients (HTCs) and the subsequent component temperature profile is handled in a single package;
- Determination of pressure drop for liquid or gas cooling (variable density, fully turbulent flow, using user-specified wall roughness);
- Rapid calculations to support exploratory studies and comparative analysis of FW PFC concepts.

THAMES requires a number of design parameters as inputs, which define the geometry, materials, hydraulic conditions and operating conditions. Figure 1 portrays the geometric parameters which are used by THAMES. In summary, these are:

- The overall FW panel height (H_{FW}) and width (L_{FW})
- The number of channels passing across the FW panel (N), and the number of channels per parallel cooling circuit (n , where $n=3$ is shown in Figure 1)
- Number of channels per de-coupled FW finger unit (note this is different from n , above). 2 or 4 channels are possible; 2 channels per finger are shown in Figure 1
- Rectangular or circular cross-section channels; both variants are illustrated in Figure 1
- The complete definition of the channel size and position, and finger dimensions, in 2-D cross-section (see Figure 1, right hand side).

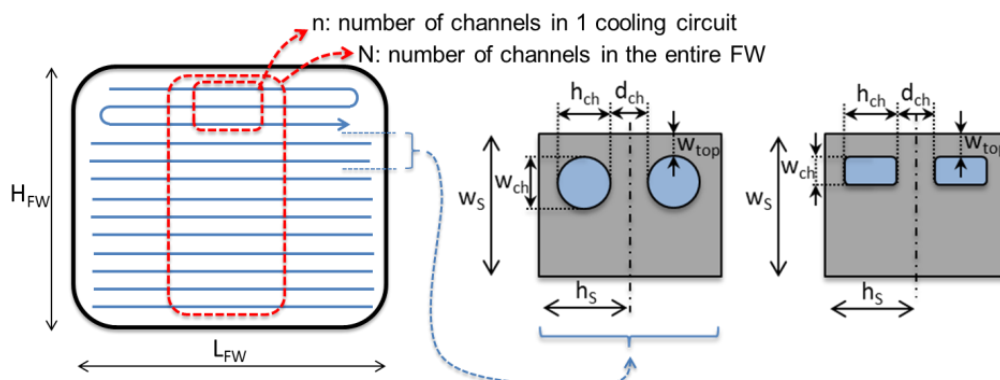


Figure 1. Geometric and cooling-arrangement design parameters of a single FW panel. In the example shown, $n=3$ and $N=13$.

Once the case to be studied is well defined, THAMES is able to launch the analysis in one of three different ‘modes’:

- 2-D Analyser Mode: used for rapid geometric and coolant parameter exploration with a 2-D finite element model coupled with thermo-hydraulic analyses. Just one single run is executed for each set of fixed parameters in 2-D (using a uniform heat flux distribution).
- 3-D Analyser Mode: if the geometry and coolant parameters are known *ab initio*, an analysis with a 3-D finite element model (again coupled with thermo-hydraulic analyses) can be run, which provides a more accurate coolant evolution along the cooling circuit and a realistic temperature distribution on the component with the option of a detailed non-uniform heat load map. Just one single run is executed for each set of fixed parameters in 3-D.
- Optimiser Mode: a design parameter of interest (e.g. outlet coolant temperature, wall thickness, heat load, etc.), can be studied by sweeping it and recording the response of the component performance. Parameters are defined with at least one degree of freedom. Several runs are executed sweeping the parameter under investigation. This mode of analysis is only available for 2-D configurations since it would not be practical using the more computationally expensive 3-D runs.

Each single run of THAMES in fact consists of an iterative loop including determination of whether or not the coolant is working as liquid water with local boiling, which requires specific correlations for HTC and Critical Heat Flux (CHF) analysis. Inputs and post-processing are connected to the ‘core function’ where the main analyses are run. Figure 2 shows and schematic view of the THAMES functions and calculation routine.

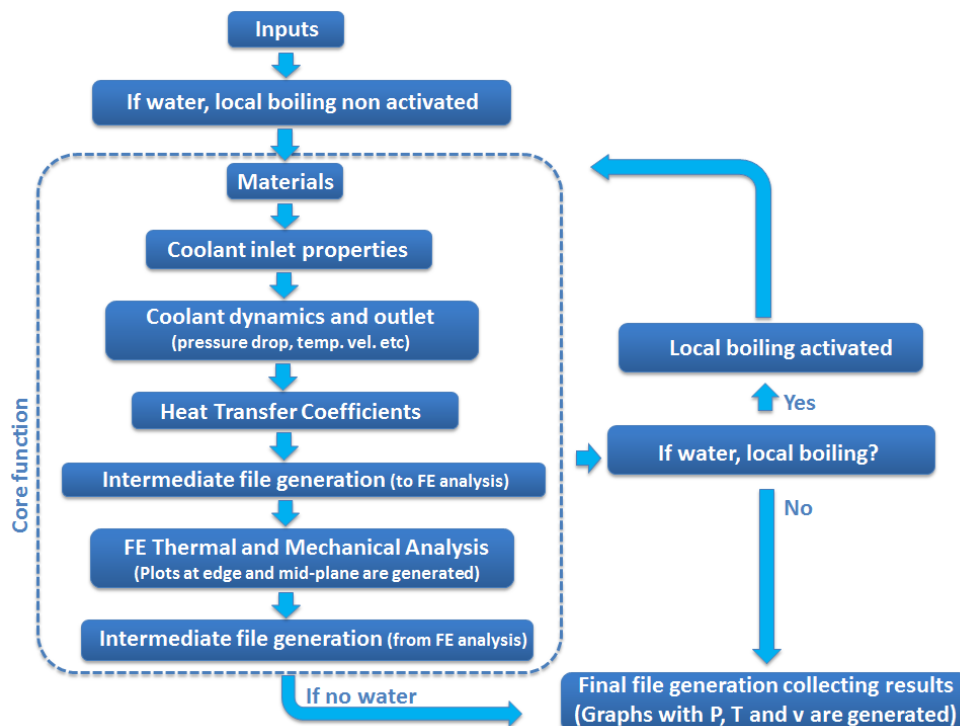


Figure 2. THAMES functions and calculation routine.

2.2. Fluid properties evolution

An important feature of THAMES is how pressure and general fluid properties are calculated along the cooling channel. This is performed by discretising the channel along its length and solving the mechanical energy equation at each small step, considering an incompressible fluid formulation even when gaseous (as the Mach number is low). However, in the case of a gas coolant, temperature and density may change significantly and so it is necessary to model the process including both conditions: incompressible formulation but with density change. A finite control volume approach is applied to every small section of the channel with density evolving from one section to the next.

Combining the mechanical energy equation and the Colebrook formula for the friction factor, we arrive at the following non-linear system to be solved iteratively at each finite step.

$$\int_i^{i+1} \frac{dp}{\rho} = \frac{p_{i+1} - p_i}{\bar{\rho}} = \frac{1}{2} \cdot (u_i^2 - u_{i+1}^2) - g h_L,$$

$$g h_L = K \frac{\bar{u}^2}{2} = f \cdot \frac{L}{D_h} \cdot \frac{\bar{u}^2}{2},$$

$$f = \frac{0.25}{\left\{ \log_{10} \left[\frac{\left(\frac{\varepsilon}{D_h} \right) + \frac{2.51}{Re \sqrt{f}} \right] \right\}^2}.$$

Where:

p : pressure	h_L : loss of height	L : length of the channel
ρ : density	f : friction factor	D_h : Hydraulic diameter
u : velocity	ε : roughness	Re : Reynolds number
g : gravity acceleration	w_s : mechanical energy	K : Loss coefficient

As a consequence, pressure (P), temperature (T), velocity (u) and density (ρ) are found at every section of the cooling circuit for a given heat input rate (\dot{Q}) (Figure 3).



Figure 3. Sketch representing the coolant evolution through the cooling circuit.

2.3. Heat transfer correlations in THAMES

Two possible fluid conditions are considered in THAMES, as listed below:

- Coolant with just one phase (gas or liquid with no local boiling).

The HTC is calculated at every position of the cooling circuit, and saved as a table to be used as input for the FE analysis. The Gnielinski correlation is chosen:

$$Nu = \frac{\left(\frac{f}{8} \right) \cdot (Re - 1000) \cdot Pr}{1 + 12.7 \cdot \left(\frac{f}{8} \right)^{0.5} \cdot (Pr^{2/3} - 1)}$$

$$HTC = Nu \cdot \frac{k}{D_h} \left(\frac{W}{m^2 K} \right)$$

Where:

Nu : Nusselt number Pr : Prandtl number k : Thermal conductivity

b. Water as coolant with local boiling (two phases).

If after running a FE analysis with liquid water, and significant local boiling is detected (wet wall temperature higher than saturated temperature at bulk pressure), the HTC is recalculated as a function of the wall temperature (with the appropriate correlations) and a new and final FE analysis is run. The methodology and correlations described in references [9] to [13] are followed. The non-linear Bergles-Rohsenow correlation is solved in order to get the temperature of onset of nucleate boiling (ONB).

$$n = \frac{2.046}{P_b^{0.0234}}$$

$$HTC_{FC}(x) \cdot (T_{ONB} - T_b) = 15500 \cdot P_b^{1.156} \cdot [1.8 \cdot (T_{ONB} - T_{sat})]^n$$

Once the wall temperature is higher than the ONB temperature, nucleate boiling is considered and:

$$q_{FC} = HTC_{FC}(x) \cdot (T_{wall} - T_b)$$

$$q_{NB}(P_b, T_{wall}) = 10^6 \cdot \left[\frac{e^{\left(\frac{P_b}{8.7}\right)} \cdot (T_{wall} - T_{sat})}{22.65} \right]^{2.8}$$

$$q_o(P_b, T_{ONB}) = 10^6 \cdot \left[\frac{e^{\left(\frac{P_b}{8.7}\right)} \cdot (T_{ONB} - T_{sat})}{22.65} \right]^{2.8}$$

$$q_{TOT} = \sqrt{q_{FC}^2 + q_{NB}^2 \cdot \left(1 - \frac{q_o}{q_{NB}}\right)^2}$$

$$HTC(x) = HTC_{TOT}(P_b, T_b, T_{wall}) = \frac{q_{TOT}}{(T_{wall} - T_b)}$$

Where:

- P_b : Bulk pressure
- T_b : Bulk temperature
- T_{wall} : Wall temperature
- T_{ONB} : Temperature of onset of nucleate boiling
- T_{sat} : Saturation temperature at bulk pressure
- $HTC_{FC}(x)$: Heat Transfer Coefficient using correlation for Forced Convection regime (no local boiling), at every 'x' position (following the length of the cooling circuit)

The final computation step is to check that the proposed coolant conditions (pressure, temperature and velocity), under the studied heat load, result in sufficient margin to avoid a critical heat flux event. The correlation Tong75 [11] is used for this purpose by evaluating the wall critical heat flux parameter (WCHF):

$$WCHF = C_f \cdot Tong75_{CHF}$$

$$Tong75_{CHF} = 0.23 \cdot f_0 \cdot \rho \cdot u \cdot h_{fg} \cdot \left[1 + 0.00216 \cdot \left(\frac{P_b}{P_0} \right)^{1.8} \cdot Re^{0.5} \cdot Ja \right]$$

Where:

- ρ : coolant density; u : coolant velocity; h_{fg} : latent heat of vaporization at bulk pressure
- $C_f = 1.25$ (*smooth tube*); 1.67 (*swirl tube*)
- $P_0 = 22.09 \text{ MPa}$; $D_0 = 12.7 \cdot 10^{-3} \text{ m}$
- $f_0 = 8 \cdot \frac{\left(\frac{D_h}{D_0} \right)^{0.32}}{Re^{0.6}}$ and $Ja = \frac{c_p \cdot (T_{sat} - T_b)}{h_{fg}} \cdot \frac{\rho_l(T_b)}{\rho_v(P_b)}$
- Experimental range of validity:
 - $2 < P_b < 4 \text{ MPa}$
 - $40^\circ\text{C} < T_{sat} - T_b < 140^\circ\text{C}$
 - $1 < u < 15 \text{ m/s}$

The accuracy of the Tong correlation is only +/- 20%, and experiments are usually required in order to obtain a correlation which well matches true observations. Due to the error and the uncertainties involved when extending the use of the correlation for different pressure, temperatures and water velocities, a CHF margin of 1.4 is considered and defined in order to avoid risk of melting [12]:

$$CHF_{Margin} = \frac{WCHF \text{ (from correlation)}}{\text{Wall Heat Flux (from thermal FEA)}} > 1.4$$

2.4. 3-D modelling in THAMES including use of a non-uniform heat load distribution

The main goal of the de-coupled FW concept is to deal with heat loads carried by particles leaving the plasma and interacting with the surface due to magnetic field line intersection. This has two very significant consequences: a highly non-uniform heat load deposition on the component and a locally high heat flux [1]. THAMES is able to run quick estimations of the behaviour of the component with 2-D FE analysis under peaked loads; however this 2-D run has limited capability since the heat transfer along the third dimension may be significant in the case of non-uniform surface heat load deposition. For this reason a 3-D analytical module has been developed in THAMES, which is able to provide much more accurate thermo-hydraulic results given complex input heat load maps.

The structure of the 3-D Analyser mode is based on an iterative process where all the thermo-hydraulic analyses are again run in Python (using the aforementioned capabilities for the 2-D Analyser module), connected to Ansys to perform the FE analysis (see Figure 4). This iterative process allows an accurate link between the thermo-hydraulic evolutions of the coolant properties along the cooling circuit with the temperature distribution on the component. Each cooling circuit is divided into sections where the heat through the wall is assessed. For each iteration the heat load at each section analysed with the 3-D FE model is used as an input to the thermo-hydraulic analysis that will provide not only the pressure and velocity evolution, but also the required HTC and bulk temperature at each position for the next FE run in the following iteration. Convergence is defined as a stable heat flow through

the channel wall between successive iterations (difference in heat flow between successive iterations is below a certain defined limit). Finally, the result is collected and plotted.

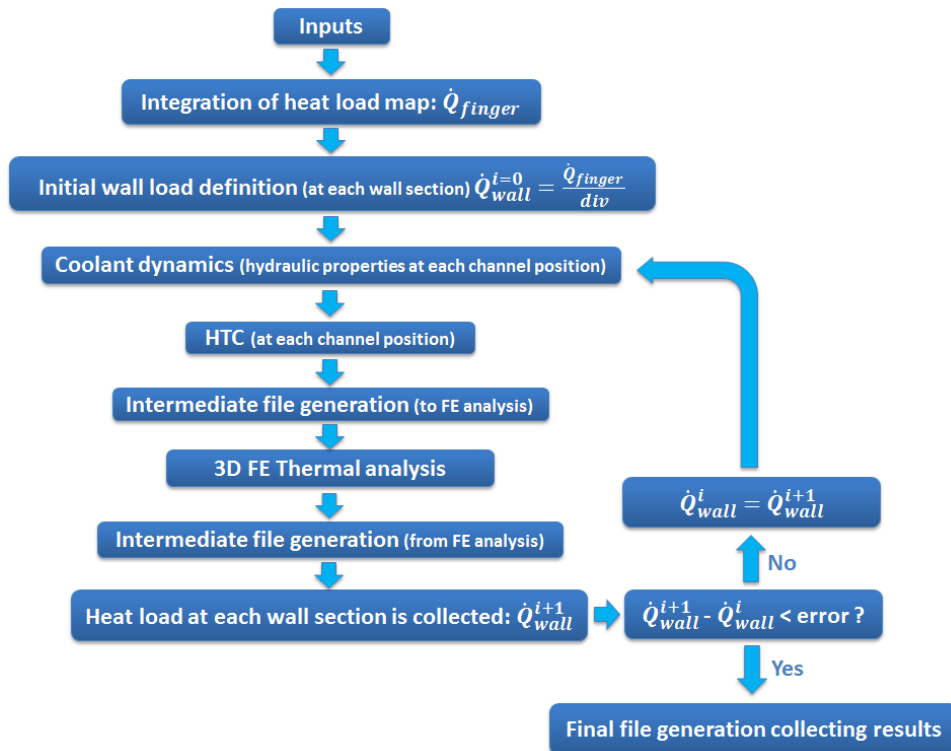


Figure 4. THAMES structure for 3-D ‘Analyser mode’ analysis.

3. Applying THAMES for exploratory design studies

This Section further develops the use of THAMES as a tool to rapidly explore different design options by modelling the thermo-hydraulic properties and combining with 2-D FE modelling (2-D THAMES mode).

In seeking the optimum design, two different methods may be applied for improving the performance of a certain proposed design: 1) modifying the cooling channel arrangements, or 2) modifying the flow turbulence. These two methods are addressed in turn below.

3.1. FW performance improvement by modifying cooling channel arrangements

The goal is to increase HTC by increasing the coolant velocity, thereby improving the heat flux removal performance. Two strategies are suggested (keeping constant the total number of channels ‘N’):

- Strategy 1: Increasing the number of channels per cooling circuit (‘n’) and keeping same hydraulic diameter (D_h) leading to higher mass flow rate per circuit, higher velocity and, as a result, higher HTC.
- Strategy 2: Keeping the same number of channels per cooling circuit (‘n’), decreasing the hydraulic diameter (D_h), but the same mass flow rate per cooling circuit and hence higher velocity and higher HTC.

As an illustration of Strategy 2, Figure 5 presents the temperature distribution for two 2-D runs in which only the hydraulic diameter is varied. Reducing D_h (in this case by reducing the channel height by 3mm) increases the flow velocity and HTC, reducing the peak surface temperature (in this case by 30 °C) and thus enabling a higher heat flux load before reaching

the 550 °C design limit. This result is for the end of a finger, i.e., inlet/outlet region, although the code also provides results at the mid-plane of the panel. THAMES is also able to consider a design option based on four channels per finger; this option is presented and described in detail in Section 6.

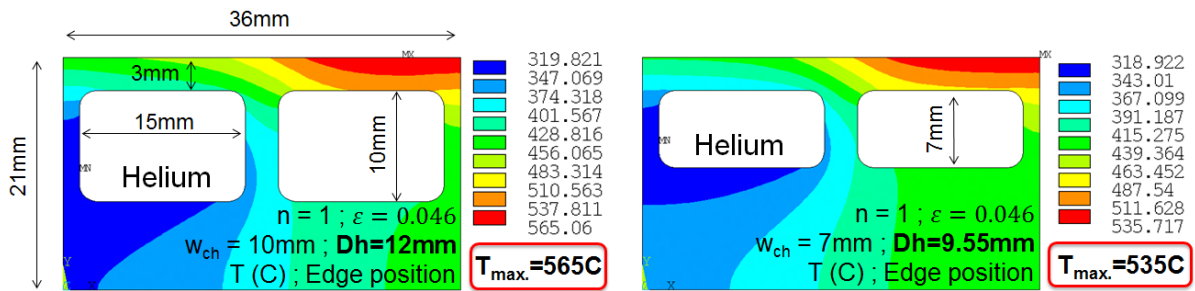


Figure 5. Temperature distribution with two different hydraulic diameters

Figures 6 and 7 show the results from THAMES when different parameters are varied and the consequences on the component performance.

Figure 6 shows the influence of the parameters ‘n’ and ‘D_h’ on maximum channel temperature and pressure drop, when 0.5 MW/m² is used as the uniform surface heat flux. The goal is to maximise the coolant temperature (for power cycle efficiency) without excessive increase in pressure drop while keeping temperatures in the structure within the limits. In Figure 6, the horizontal dashed red line represents the upper temperature limit imposed by the Eurofer material, which is taken to be 550°C because of the potential for creep failure.

Figure 7 shows the influence of the parameters ‘n’ and ‘D_h’ on structural temperature when a coolant temperature rise from 300 °C to 380 °C is maintained. The goal is to maximise the peak heat flux without excessive increase in pressure drop while maintaining acceptable temperature in the structure (again, limited to 550 °C).

In conclusion, it is seen that the pressure drop is much more sensitive to the parameter ‘n’ (number of channels per cooling circuit) than to D_h (the hydraulic diameter). However, it is possible to improve the cooling performance by increasing slightly ‘n’ and/or by decreasing moderately the hydraulic diameter, and still keeping an acceptable temperature distribution in the component. An increase of 20°C on the outlet coolant temperature or an increase of 0.2 MW/m² are achievable (keeping a low pressure drop increase and 550°C as maximum structure temperature) by using n=2 and D_h=8.5mm. Any further increase in ‘n’ (i.e., n=3) would result in a prohibitive pressure drop increase.

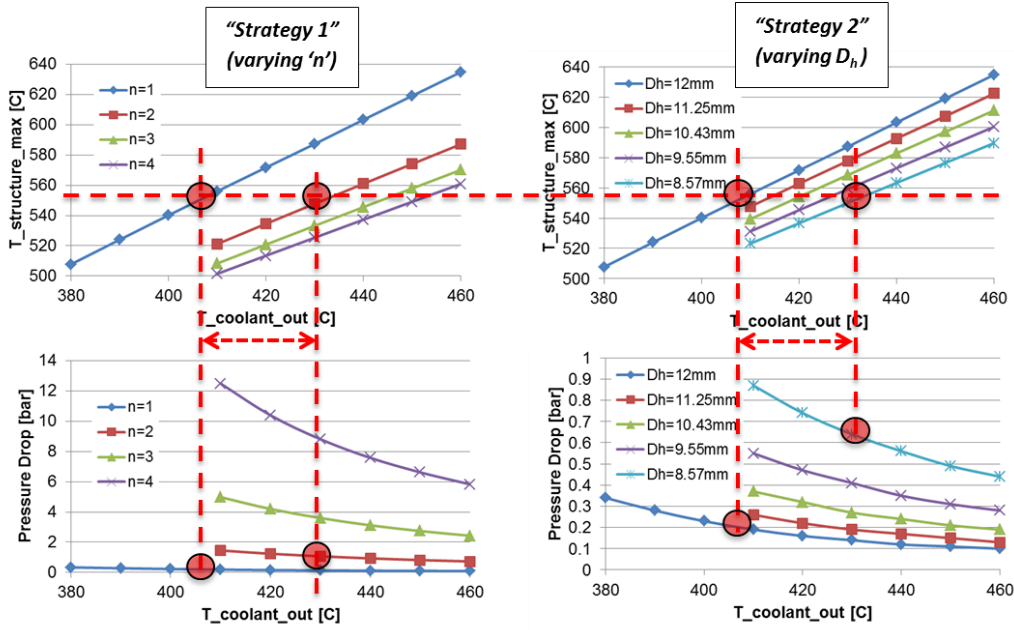


Figure 6. The effect of n and D_h on peak structural temperature and pressure drop, for a fixed uniform surface HF of 0.5 MW/m^2 .

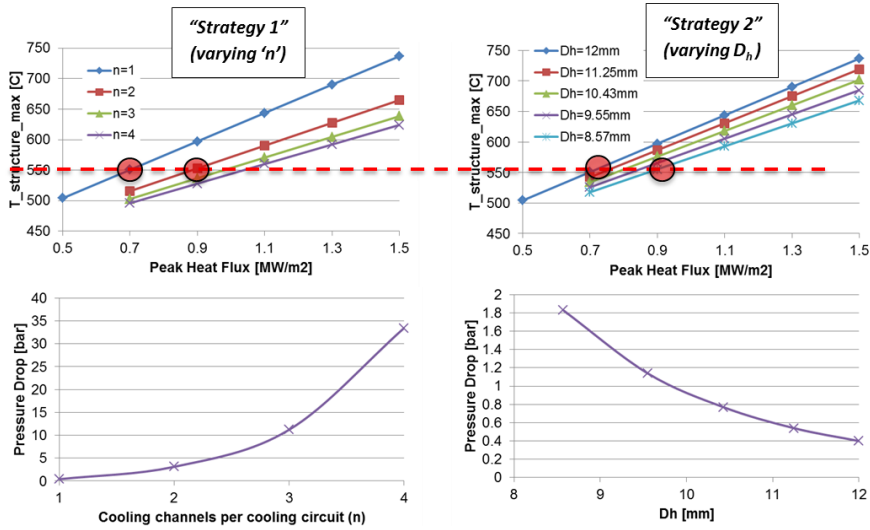


Figure 7. The effect of n and D_h on peak structural temperature and pressure drop, for a fixed coolant temperature rise (300°C to 380°C).

3.2. FW Performance improvement by increasing turbulence

THAMES is able to explore FW enhancement when the design includes features intended to increase channel turbulence, which increases the HTC but also the pressure drop. There are two main ways of increasing the turbulence: 1) by changing the channel technology, and 2) by increasing the surface roughness.

As mentioned above, circular, rectangular and swirl tubes are included in THAMES as channel technology options, and these can be either smooth or given a specified wall surface roughness. Figure 8 presents contour plots obtained by running in THAMES two cases with both helium and water as coolant. The first case (Figure 8 left) is modelled with smooth channels while the second one (Figure 8 right) includes channels with a roughness of 0.046

mm (a typical value for as-received commercial steel pipes). A constant and uniform surface heat flux of 0.5MW/m^2 is assumed in both cases. As it is seen, the reduction in temperature may be substantial when channel roughness is taken into account.

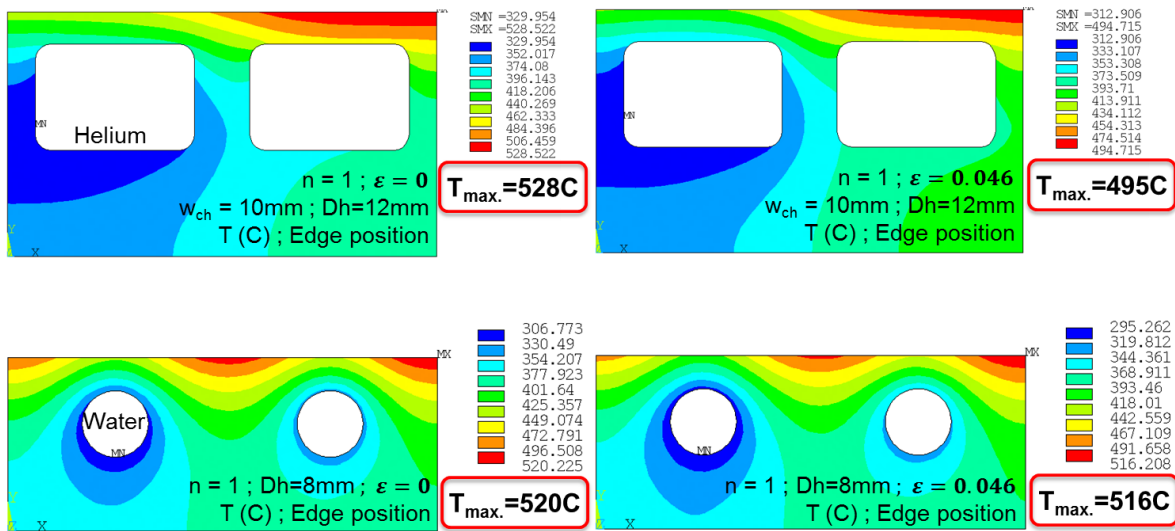


Figure 8. Comparing THAMES results: smooth channels vs. channels with roughness

4. Design basis for the proposed FW ‘finger’ concept

The present Section specifies the design parameters giving basis to the proposed concept described in Section 5. Section 6 presents results after analysis using 2-D and 3-D THAMES.

The design parameters are classified as those that define the geometry, those that define the hydraulic conditions, and those that define the loading conditions. Further, it is necessary to define the coolant, the heat load map (for the refined 3-D analysis), and the materials. The parameters listed in Table 1 are chosen for analysis using THAMES, first in 2-D and then in 3-D mode.

The heat load map (heat flux density distribution over the FW finger surface) is proposed as a constant base of 0.5MW/m^2 with a peak of 2MW/m^2 at the edge (see Figure 9). This heat flux map is currently arbitrary since a DEMO wall load specification is still under development, but using such a non-uniform heat load will test the response of the component to peaked loads and how well the design is able to distribute heat from hotter areas to cooler areas. A highly peaked heat flux distribution is expected due to the nature of off-normal plasma events and the effect of gaps and assembly tolerances.

Table 1. Design parameters for the FW finger concept.

	<i>Parameter</i>	<i>Specification</i>	<i>Comments</i>
Design and geometry	PFC materials	Tungsten (armour) and Eurofer (structure)	Low activation desired
	Coolant	Helium	The decision of helium or water coolant remains an open design choice*, but helium is used in the present study.
	FW dimensions	$L_{FW}=1$ m, $H_{FW}=1.5$ m (FW panel width and height, see Figure 1)	This means that the length of each channel is 1 m.
	Total number of FW channels	88	
	Hydraulic topology	2 channels in series i.e., $n=2$ (referring to Figure 1)	Gives reasonable pressure drop and good thermo-hydraulic performance (see Section 3.1)
	Channel cross section	$15 \times 10 \text{ mm}^2$	These are typical He channel dimensions. A lower D_h while $n=2$ would give excessive pressure drop.
	FW Eurofer front face thickness	1 mm	i.e., thickness between W-Eurofer bond and inner channel wall
	Tungsten armour thickness	2 mm	
Hydraulic conditions	Channel roughness	0.046 mm	
	Inlet temperature	300 °C	
	Outlet temperature	350 °C	
	Inlet pressure	80 bar	
Loading	Nuclear heating	10.93 MW/m^3	
	Surface Heat Flux	0.5 MW/m^2 (2-D analyses) or 2 MW/m^2 peaked distribution (3-D analyses)	Heat load map shown in Figure 9.

* Both helium and water are proposed as coolants of the different blanket concepts in the design of DEMO. Although water can achieve superior heat transfer rates, it causes corrosion of the Eurofer coolant channels, and the channel wall may need to be made significantly thicker (to give sufficient margin) than a helium cooled design. Indeed the corrosion rate from water in the nucleate boiling regime (in which the HTC is highest) may be highly aggressive, although appropriate R&D is needed to quantify this. Another advantage of helium as coolant is the typical coolant pressure adopted by designers is substantially lower than for pressurised water (80 bar vs. 155 bar, respectively), which roughly halves the primary membrane stress in the FW structural material. Hence, helium being chemically inert and having a lower pressure both potentially allow for a thinner FW front face which enables a higher heat flux before reaching thermal limits.

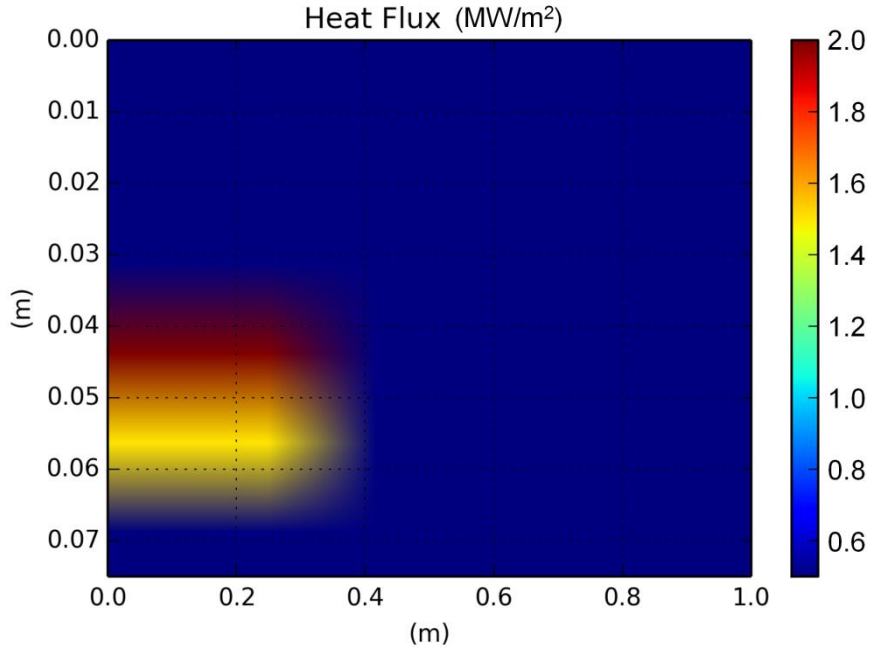


Figure 9. Input heat flux map applied to the de-coupled FW finger (vertical axis: finger width, horizontal axis: finger length).

Regarding the parameters in Table 1, the following rationale is applied. The total number of channels (88) is a consequence of the assumed FW size. The FW is hydraulically arranged with 2 channels in series as this simplifies the FW design, and we have shown that the $n=2$ case increases HTC and outlet temperature without excessive penalty in terms of pressure drop (Section 3.1, above). The FW Eurofer front face thickness (i.e., distance between the W-Eurofer bond and the inner channel wall) has a drastic influence on the maximum temperature reached in the Eurofer. A thin wall is needed to limit the peak temperature, but it has to be thick enough to withstand primary and secondary stresses. Since helium is chosen as coolant, 1 mm thickness is assumed as a good starting value for the present study.

The armour thickness has been chosen to be 2 mm. This is an arbitrary value and further studies on plasma-wall erosion will be required for its definition. A typical channel roughness on commercial steels is assumed (0.046 mm). The inlet temperature is selected in order to avoid the shift of Eurofer DBTT under irradiation. The selected outlet temperature is relatively low in order to lower the Eurofer maximum temperature and hence maximise the allowable heat flux, although this is clearly a compromise as too low an outlet temperature would result in prohibitively large pressure drop. The nuclear heating is selected following reference [15].

5. Design Description of the proposed de-coupled FW finger concept

5.1. Main features of the de-coupled FW finger design

As described in Section 1.1, a key advantage of a de-coupled FW concept based on fingers is the reduction in thermal stress in the discrete components compared to a continuous (integrated) blanket-FW panel. To illustrate this, Figure 10 shows that an individual FW finger comprising two cooling channels (right) has a considerably lower thermal stress than the continuous integrated FW (left). This is a simple reference case (see [2]) with both designs having a 0.5 MW/m^2 uniform surface heat flux and equivalent hydraulic conditions, but the key difference is that the integrated FW has symmetry applied to the lateral faces (and

constraints representing the blanket stiffening grids), whereas the de-coupled FW design has lateral faces which are free to expand and deform.

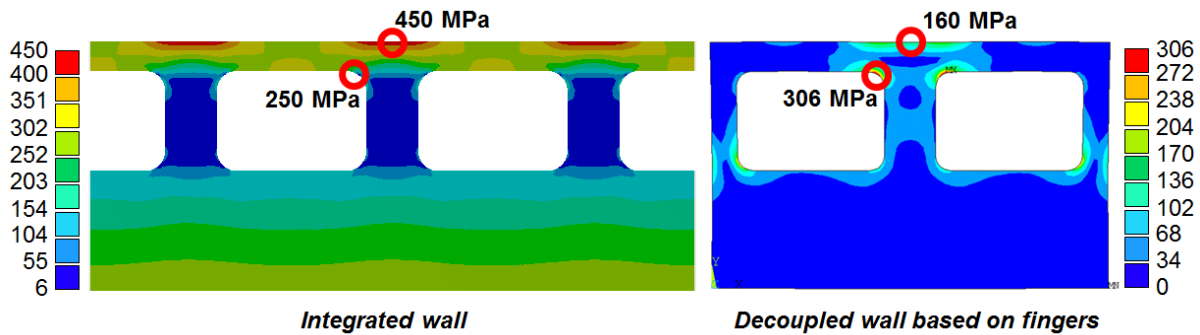


Figure 10. Equivalent (Von Mises) stress comparison for an integrated FW (left) and de-coupled FW (right) (contour units: MPa).

A consequence of splitting the FW into a number of components is an increase in the number of edges exposed to particles coming from the plasma that could potentially cause damage. How these edges are protected is something that strongly depends on the orientation of the finger. Since, in the global sense, field lines follow mainly the toroidal direction, fingers orientated toroidally are strongly preferred. A gentle curvature is provided to each finger surface in the poloidal direction in order to shadow the edges of neighbouring fingers (see Figure 11).

As outlined in Section 4, it is expected that 10 x 15 mm rectangular channels with two channels in series ($n=2$) maintains reasonable pressure drop while giving good thermo-hydraulic performance. For symmetry of cooling performance across the width of the component, we use two cooling circuits per finger (see Figure 11). There are therefore four cooling channels per finger, with the two inlets in the centre and the two returns at each side.

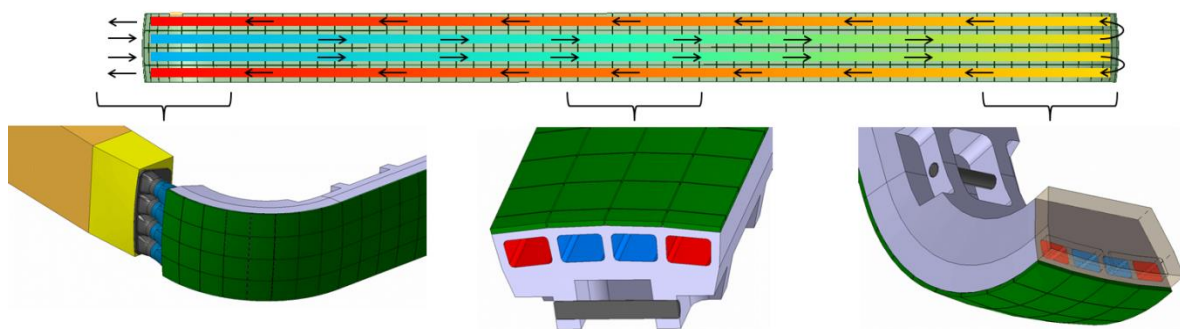


Figure 11. FW hydraulic arrangement: inlet/outlet in the left; closing caps (turning the flow direction 180°) on the right.

The proposed design comprises three main components: fingers, transition piece and the manifold side boxes (see Figures 12 and 13). The manifold side box delivers coolant to and from the FW (see details in Section 5.3), while the transition piece links this manifold to the finger coolant channels. The cooling circuits are closed with one side connected to the transition piece via weld stubs (Figure 13), and with the opposite end welded to closing caps which arrest and turn the flow by 180° (Figure 11, right). This compact arrangement allows appropriate thermal expansion on the finger length direction (by using an appropriate

attachment design, presented in Section 5.2), and avoids the need for coolant feed pipes on both sides of the BB box (by using an appropriate manifold box design, presented in Section 5.3).

A detailed design proposal should of course consider a specific blanket location in the DEMO main chamber in order to choose the right FW panel size and loading conditions that would drive the FW finger design parameters. The design here proposed (and later analysed, in Section 6), follows the parameters described at Section 4 i.e., assuming 88 cooling channels and a FW size of 1x1.5m.

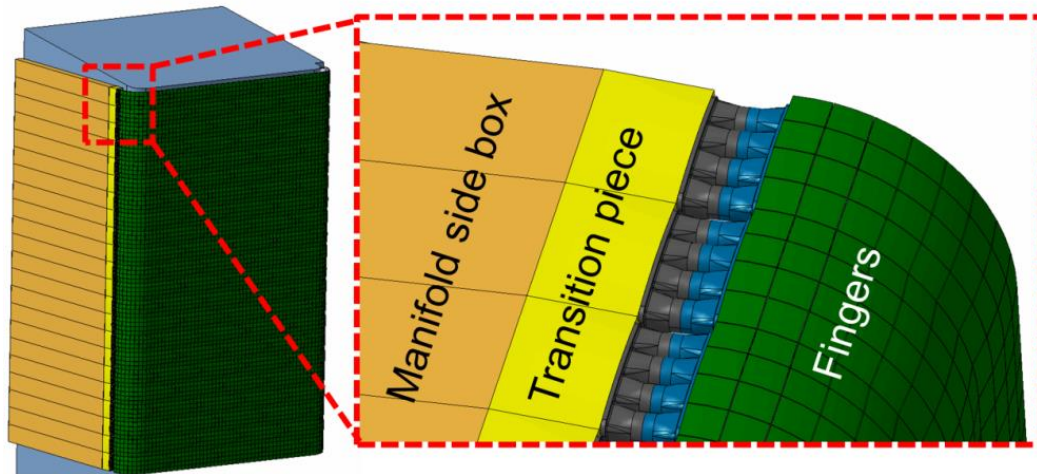


Figure 12. De-coupled FW Finger concept, showing Fingers mounted on a BB module and the coolant feed/manifold arrangement.

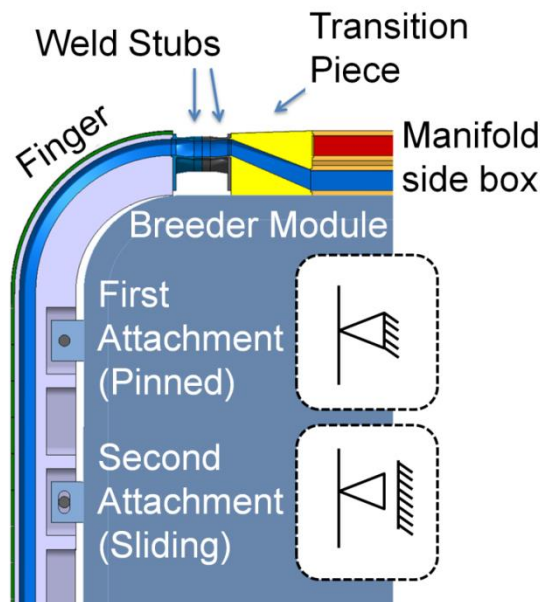


Figure 13. De-coupled FW finger components and attachment lugs (radial-toroidal cross sectional view).

5.2. Attachment design

An attachment concept has been developed in conjunction with the manifold design. The FW is not designed to be remote handled inside the machine (unlike in ITER, where remote maintenance of the FW is planned). Instead the FW attachment design has to provide

capability for exchanging it in a hot cell environment (while preserving the BB). The current DEMO baseline design does not have a FW replacement capable hot cell. It would be an economic decision whether to include this capability in the hot cell or to replace the entire BB but it should be technically feasible.

A strong driver is to eliminate the need for flexible (and easily damaged) components such as bellows whilst allowing the high heat flux component freedom to expand and deform (and so minimise thermal stress). The design consists of attachment lugs fitted to the breeder Blanket module (see Figures 14 and 15). The first lug (starting from the edge closest to the manifold) has a circular location hole to fix the high heat flux component with a pinned connection (Figure 13). All the other lugs onwards have slotted holes to produce a sliding joint. Since the finger is designed ending at the opposite edge to the manifold, as shown in Figure 15, this attachment concept allows the high heat flux component to expand and reduces thermal stress in the finger and manifold. Critically, the FW attachment scheme does not rely on preloading features, as on ITER, as such a preload would significantly decrease with time under exposure to the DEMO neutron environment.

The design of the attachment is likely to be driven by the electromagnetic loads. Section 5.4 presents a preliminary electromagnetic analysis exploring the mechanical loads that would be transmitted to the attachments.

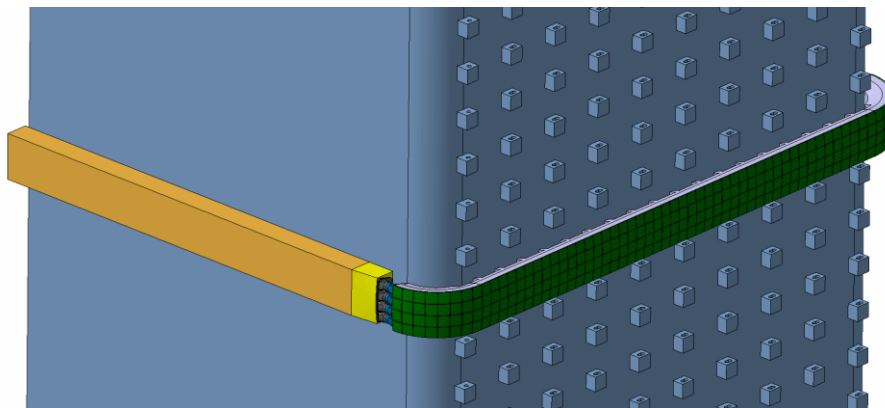


Figure 14. FW finger and attachment lugs on the front face of the BB.

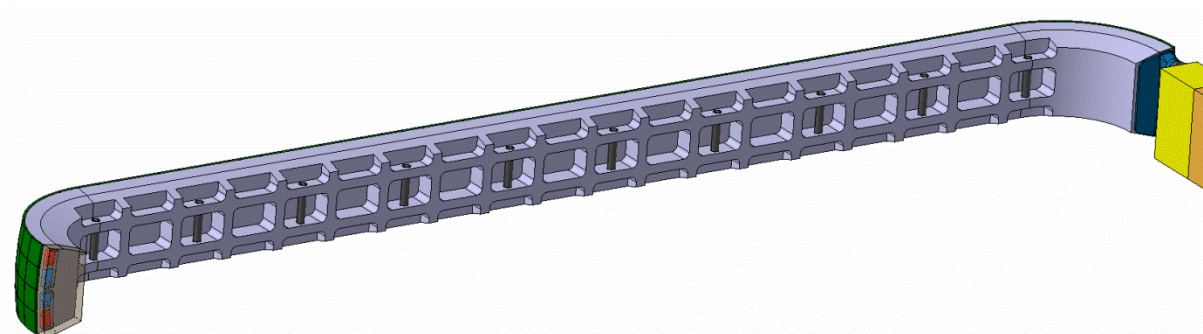


Figure 15. Rear view of a complete de-coupled FW finger.

5.3. *Manifold design*

A manifold design concept has been proposed and is here described. The manifold will be used to route coolant from the blanket segment back supporting structure to the front of the Blanket, each providing the FW coolant inlet and outlet for a single finger. Figure 16 shows the main components of the manifold: manifold side box, transition piece, and weld stubs.

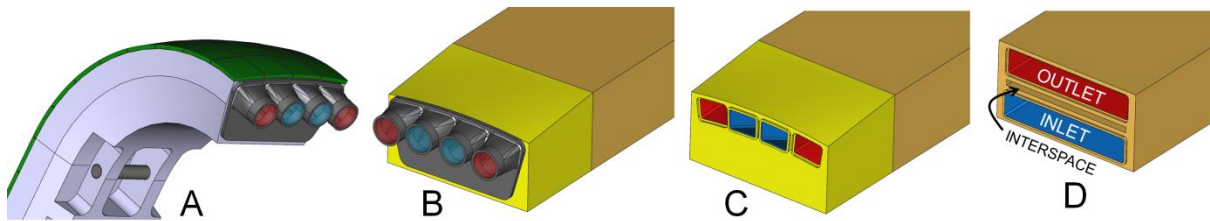


Figure 16. Manifold concept. A: finger inlet/outlet region and weld stubs; B: manifold side weld stubs; C: transition piece; D: manifold side box.

The function of the manifold side box is to transfer coolant to and from the back supporting structure to the high heat flux component with a minimum pressure drop. To facilitate this, a large rectangular cross section has been chosen (see Figure 16, D). There is an interspace between the inlet and the outlet chambers aiming to reduce heat transfer between them. A small pocket is machined into the outlet coolant chamber, and there is a small protrusion from the inlet chamber. The transition piece (Figure 16, C) is located and sealed using an interface fit on these protrusions/pockets. A perimeter electron beam weld is then completed. Regarding the manufacturability, the transition piece can be manufactured by either 3-D printing or using conventional machining.

The weld stubs (Figure 16, B) enable the final connection between the high heat flux components and the manifold by using an orbital welding head. The weld stubs can be electron beam welded into the respective components before final assembly. During final assembly an orbital welder can make the final weld once each high heat flux component has been attached to the blanket module.

The manufacturing concept is in its infancy and will need further refinement as the design activity progresses. In particular the clearances around each component may need to be increased to improve welding access, together with development of the inspection regime post welding for quality assurance.

5.4. Preliminary EM analyses

A preliminary electromagnetic analysis has been conducted to assess the feasibility of the proposed attachment design with respect to the possible forces as a consequence of electromagnetic events. Moreover, this preliminary analysis is an key factor in deciding the orientation of the fingers.

Figure 17 shows the component under analysis, i.e., one finger with its corresponding manifold. The analysis was conducted with the finger oriented 1) toroidally (as in Figure 17) and 2) poloidally (rotated through 90°). The electromagnetic loads on the component were computed using both an analytical and numerical approach; the analytical model is applied on solid rectangular blocks of equivalent cross section and the numerical model (a FE analysis) is applied on the geometry shown in Figure 17 (albeit with some simplification applied to enable FW meshing, etc).

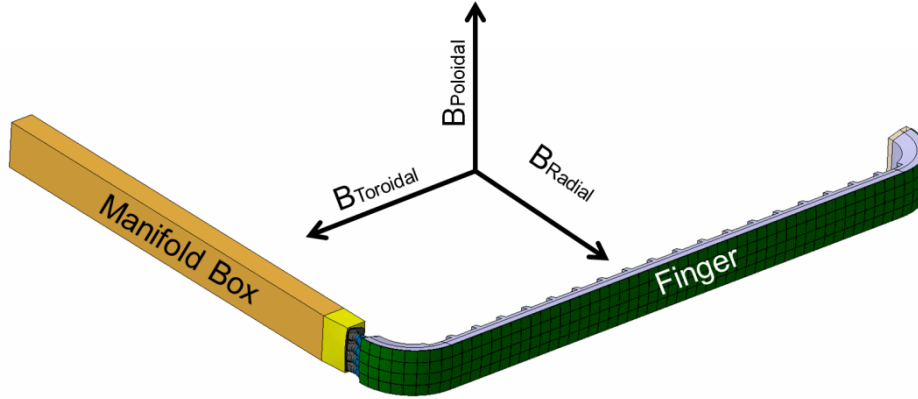


Figure 17. Finger and manifold box in toroidal orientation for the EM analysis.

In order to estimate the mechanical loads generated during a disruption we considered the ITER scenario described in [16] as a reference, i.e., the poloidal field decaying linearly from 1.8 T to 0 T in 30 ms (major upward disruption, which is the worst-case scenario and gives the largest radial torque). The toroidal magnetic field is assumed constant during the disruption and equal to 8.8 T. The radial field is assumed to be zero. The induced eddy currents were calculated assuming quasi-static (the displacement current term in Maxwell's equations is neglected) and induction-less (the magnitude of the field generated by the induced currents is small compared to the applied field) approximations. The electrical conductivity of Eurofer was taken to be $\sigma = 1.35 \text{ MS/m}$. The result is summarised in Table 2.

Table 2. Summary of EM analysis result (radial torque).

Model	Radial torque with finger in poloidal orientation	Radial torque with finger in toroidal orientation
Analytical model	1319 Nm	557 Nm
FE model	1230 Nm	398 Nm

The main contributor to the radial torque is the current induced on the manifold box. When the finger component is oriented poloidally the manifold box presents a large poloidal-facing area where the poloidal field variation can induce large currents. However, when the finger is oriented toroidally the poloidal-facing area of the manifold is greatly reduced (because of the aspect ratio of the manifold cross section) and, as a consequence, the induced currents and the torques are considerably lower. Thus, we can conclude that the toroidal orientation (as in Figure 17) is preferable from the EM (disruption load) point of view as well as being preferable with respect to charged particle heat loads, as discussed above.

6. THAMES results for the proposed de-coupled FW finger concept

This Section demonstrates how the THAMES 2-D and 3-D Analyser modes have been used in combination to analyse the design of the de-coupled FW based on fingers as presented in previous Sections 4 and 5. As a result of the chosen parameters and design configuration, THAMES provides the 2-D and 3-D temperature distribution as well as the coolant properties evolution along the cooling circuits. Figures 18, 19 and 20 summarise the result, as described next.

Figure 18 shows 2-D analyser temperature results on a cross section at the inlet/outlet end of the finger. The input distribution of heat flux across the surface results in a temperature peak above the right-most (outlet) channel of 564°C. With the 2-D assumption, the component is at (in fact slightly above) the design limit of 550°C with the imposed loading. However, these results can be regarded as conservative, as is expected since the 2-D model does not simulate the longitudinal transfer of heat from a heat flux peak to the cooler region of the structure.

Also presented in Figure 18 is the temperature field, at the same inlet/outlet station, from the 3-D THAMES model (which uses the full heat flux map in Figure 9). This result demonstrates the response of the finger component to a heat flux peak ('hot spot') of 2 MW/m². The 3-D THAMES accounts for longitudinal as well as transverse heat dissipation, and the resulting temperature peak of 465°C is well within the design limit of 550°C. Consequently, the component may be able to sustain heat flux peaks of greater than 2 MW/m². This is a notable result, since we know in reality that the wall heat flux will be highly peaked (because of plasma behaviour and the effect of gaps/assembly tolerances) but from the results shown here we see that considerable localised peaks can be tolerated with respect to structural material temperature.

Figure 19 shows the expected non-linear evolution of the He coolant temperature, which also means a non-linear evolution of the velocity (since the density decreases with the temperature and the mass flow rate is conserved). Both temperature and velocity increase faster where the higher heat flux is located, i.e., cooling circuit 2. For the same reason, circuit 2 receives the highest temperature and velocity in the outlet (note that the specified outlet temperature of 350°C is the result of mixing both circuits flows). However, also in Figure 19 it is seen that the pressure evolves linearly without a peak due to the peak heat flux (one of the channels presents slightly higher pressure drop than the other due to the higher velocity).

Figure 20 shows the temperature distribution on the Eurofer component, i.e., excluding the tungsten tiles. The 'hot spot' can be observed just under the area where the peak heat flux has been applied. Clearly, a structural material with higher thermal conductivity would improve the spatial distribution of this hot spot, increasing the heat transfer from the surface to the cooling channels and decreasing the maximum temperature.

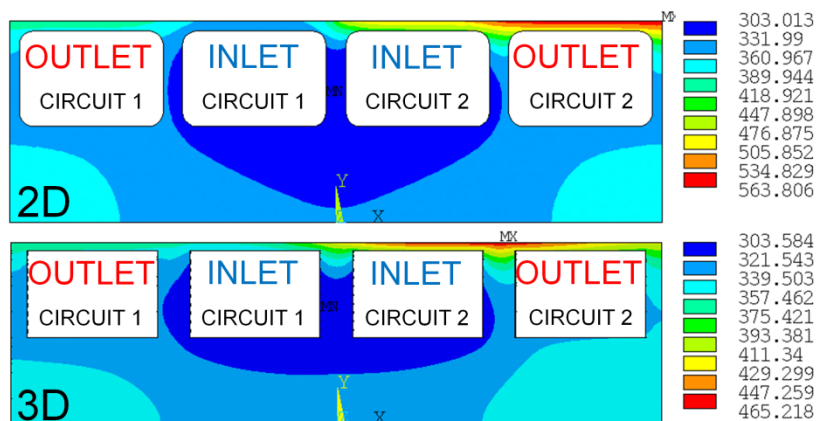


Figure 18. Comparison of temperature results (°C) between 2-D (upper) and 3-D (lower) analyses at the edge of the finger (excluding results on tungsten tile). N=4 and n=2.

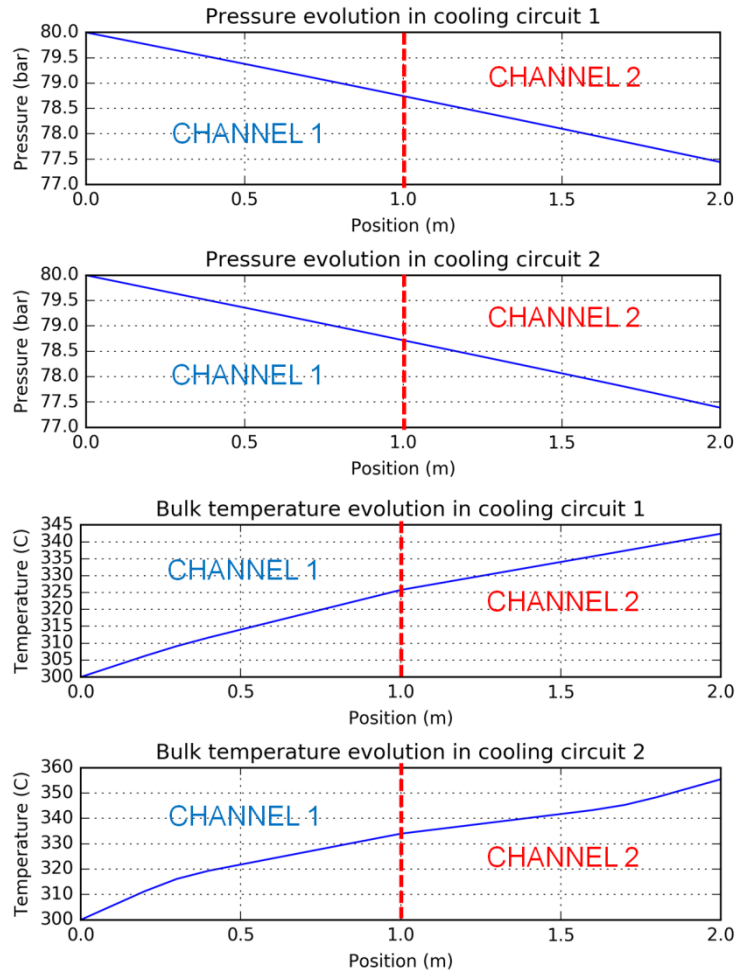


Figure 19. Pressure and bulk temperature evolution in cooling circuit 1 & 2 (left and right side respectively in Figure 18).

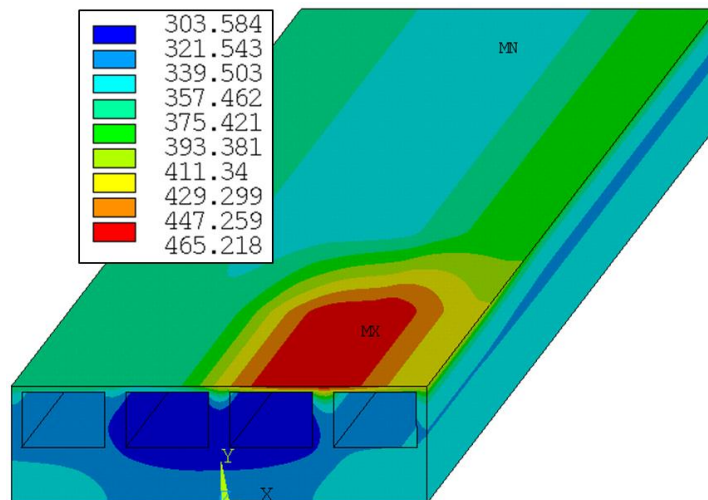


Figure 20. 3-D view of the temperature distribution (excluding tungsten tile), when using the 2 MW/m^2 peak heat flux “hot spot” map (Figure 9).

Of course, the heat flux map assumed in this study is arbitrary, and the extent to which the design is robust to heat flux peaks must be further studied. Also critical is the structural performance of the design; structural analysis must be performed to understand whether structural failure modes (e.g., plastic collapse, fatigue, progressive deformation) give lower heat flux limits than the temperature limit used here.

7. Conclusions and future work

This paper has presented the concept of a de-coupled first wall for the European DEMO. The motivation for a FW de-coupled from the blanket system is to reduce FW thermal stress, hence raising the heat flux limit, and to protect the blanket modules from plasma off-normal events. The need to explore the design space of such a proposal has led to the development of a bespoke thermo-hydraulic calculation tool. This tool is called THAMES, and is able to quickly analyse different geometrical or fluid regime cases, allows sweeping of key parameters, and includes the capability to validate the concept with more sophisticated 3-D analysis accounting for a non-uniform surface heat flux map. Each THAMES run comprises thermo-hydraulic analyses deriving coolant property evolution from the inlet to the outlet, and a coupled thermal and structural FE analysis.

The proposed de-coupled FW concept consists of individual helium cooled “fingers”. Although the use of Eurofer as structural material limits the heat flux handling capability to a modest level, it is shown that the design would be able to withstand considerable heat flux peaks or “hot spots”, potentially higher than 2 MW/m^2 . This is important as it is expected that the FW heat flux distribution will be highly peaked and it is vital to quantify what level of peaking can be tolerated by plasma facing components. A design concept of the de-coupled finger, its attachment to the blanket module, and solutions for coolant delivery are presented. A preliminary electromagnetic analysis has been reported in order to scope the loading conditions on the attachment, and confirms that a toroidal orientation of the fingers is desired.

Future work on this concept will involve performing more detailed structural assessments against a range of failure modes to improve understanding of the engineering heat flux limit of these components. A computational fluid dynamics analysis should be performed to evaluate the pressure drop due to the complex fluid flow through the manifold-finger interface and the fully reversing coolant return feature of the finger.

Acknowledgements

This work has been carried out within the framework of the EUROfusion Consortium and has received funding from the Euratom research and training programme 2014–2018 under grant agreement No. 633053 and from the RCUK Energy Programme (grant No. EP/I501045). To obtain further information on the data and models underlying this paper please contact PublicationsManager@ccfe.ac.uk. The views and opinions expressed herein do not necessarily reflect those of the European Commission

References

- [1] G. Federici et al, “Overview of EU DEMO design and R&D activities”, *Fus. Eng. Des.* 89 (2014), 882-889.
- [2] G. Aiello et al., “Development of the Helium Cooled Lithium Lead blanket for DEMO”, *Fus. Eng. Des.* 89 (2014) 1444–1450.

- [3] J. Aubert et al., “Optimization of the first wall for the DEMO water cooled lithium lead blanket”, *Fus. Eng. Des.* (2015), in press.
- [4] F. Arbeiter et al., “Thermohydraulics of helium cooled First Wall channels and scoping investigations on performance improvement by application of ribs and mixing devices”, *ISFNT-12*, 2015.
- [5] P.K. Domalapally et al., “Assessment of Hypervapotron Heat Sink Performance using CFD under DEMO Relevant First Wall Conditions”, *ISFNT-12*, 2015.
- [6] R. Lindau et al., “Present development status of EUROFER and ODS-EUROFER for application in blanket concepts”, *Fusion Engineering and Design*. 75–79 (2005), 989–996.
- [7] T. Barrett, et al., “Progress in the engineering design and assessment of the European DEMO First Wall and Divertor plasma facing components”, *Fusion Engineering and Design*, 109-111, Part A (2016), 917-924.
- [8] G. Pérez, R. Mitteau, R. Eaton, R. Raffray, et al., “Investigation on bonding defects in ITER first wall beryllium armour components by combining analytical and experimental methods”, *Fusion Engineering and Design*, 2015.
- [9] T. D. Marshall, D. L. Youchison and L. C. Cadwallader, “Modeling the Nukiyama curve for water-cooled fusion divertor channels,” *Fusion Technology*, 2001.
- [10] J. Boscary, M. Araki, J. Schlosser, M. Akiba and F. Escourbiac, “Dimensional analysis of critical heat flux in subcooled water flow under one-side heating conditions for fusion application,” *Fusion Engineering and Design*, 1998.
- [11] L.S. Tong, “Boiling Crisis and Critical Heat Flux”, USAEC, Washington, DC, 1972.
- [12] L.S. Tong, “A phenomenological Study of Critical Heat Flux”, in: *ASME Paper 75-HT-68*, ASME, National Heat Transfer Conference, San Francisco, CA, 1975.
- [13] G. Pérez, R. Mitteau, “Optimized mass flow rate distribution analysis for cooling the ITER Blanket System”, *Fusion Engineering and Design*, 2014.
- [14] F. Arbeiter, et al., “Thermal-hydraulics of helium cooled First Wall channels and scoping investigations on performance improvement by application of ribs and mixing devices”, *Fusion Engineering and Design* (in press).
- [15] J-C. Jaboulay, G. Aiello, J. Aubert, R. Villari, U. Fischer, “Comparison over the nuclear analysis of the HCLL blanket for the European DEMO”, *Fusion Engineering and Design*, 2016.
- [16] Y. Zhai, R. Feder, A. Brooks, M. Ulrickson, C.S. Pitcher, G.D. Loesser, “Electromagnetic analysis of ITER diagnostic equatorial port plugs during plasma disruptions”, *Fusion Engineering and Design*, 2012.